Proceedings of the ASME 2013 32nd International Conference on Ocean, Offshore and Arctic Engineering
OMAE2013
June 9-14, 2013, Nantes, France

OMAE2013-10660

SCOUR ASSESSMENT AND MEASUREMENTS FOR PILE-SUPPORTED WIND TURBINE FOUNDATIONS

Bruno Stuyts
Cathie Associates
Diegem, Belgium

David Cathie
Cathie Associates
Diegem, Belgium

Yi Xie
Advanced Geomechanics
(formerly Cathie Associates)
Perth, WA, Australia

ABSTRACT

With the rapid development of offshore wind energy in Europe, a large number of piled structures are being installed. In areas with sandy seabed conditions, erosion of sediment by the actions of wave and current can negatively influence foundation capacity. An accurate prediction model of scour around the piles is therefore required. Well-accepted scour prediction methods exist; both for the equilibrium scour depth and the time scale of scour [1] around single piles. These standard formulas have been combined with metocean data and a hindcasting model to calculate the expected scour depth around piles of wind turbine tripod foundations. Other causes of scour, such as pile-pile interaction, effect of proximity of structural members to the seabed, and seabed mobility were also assessed in order to determine the amount of global scour to be considered. The scour predictions were compared to measurements taken at an offshore wind turbine foundation at Park Alpha Ventus (PAV) in the German North Sea [2]. The data showed very good agreement with the measured scour around the piles. Both the equilibrium scour depth and time scale of scour were well predicted using the hindcasting model. The measured scour below the central column of the tripod structure exceeded expectations; this is believed to be due to a pumping effect during storm episodes. Finally, the effect of scour on the vertical effective stress around the tripod piles was assessed with a finite element model. Local scour had an important effect while scour below the centre of the structure had a much more limited effect. Considering the combined effects of multiple pile interaction, scour below the central column, and making an allowance for seabed mobility, an equivalent global scour depth for pile capacity calculations was established.

INTRODUCTION

Offshore wind energy is rapidly developing into a major source of renewable energy in Western Europe with up to 3GW of installed capacity in April 2011 and a further 2.5GW under construction [3]. Several North Sea wind farm sites are positioned in glacial deposits with loose to medium dense layers of cohesionless soil at the surface. Piled foundations installed in such soil conditions will inevitably be subject to scour [4].

Scour assessment methods were developed in the past for offshore Oil & Gas infrastructure and can be applied to foundations for offshore wind turbines. This paper shows how calculated equilibrium scour depths and time scales of scour can successfully be combined with a hindcasting model to obtain good predictions. An example for a piled tripod in the German Sector of the North Sea is presented.

For piled foundations, scour will have an impact on the axial pile foundation capacity. The method proposed by the American Petroleum Institute (API) [5] is compared to numerical modeling results. The numerical model takes the scour pits around each of the piles into account and determines the effect of scour on the effective stresses at the pile-soil interface. The results show that the API recommendation is a conservative approximation.

NOMENCLATURE

d_{50}	Median grain size
s	Specific gravity of solid sand particles
θ	Shields parameter
u*	Bed shear velocity
g	Acceleration of gravity
θ_{cr}	Critical Shields parameter
u^*_{cr}	Critical bed shear velocity
$\bar{U}$	Depth-averaged current velocity
$\bar{U}_{cr}$	Critical depth-averaged current velocity
h	Water depth
H_s	Significant wave heights
KC	Keulegan-Carpenter number
u_{max}	Maximum value of orbital velocity
B	Bracing diameter
D	Pile diameter
T_z	Wave period
S_{eq}	Equilibrium scour depth
t	time
T_{char}	Characteristic time scale of scour

SEDIMENT MOBILITY

Seabed material

Cohesionless soils are subject to erosion due to the action of currents and waves. The medium grain size (d_{50}) of the particles and the specific gravity of the solid particles (s) are the principal input parameters for sediment mobility calculations.

In the example for a foundation at PAV presented in this paper, the seabed consisted of fine to medium sand with a median grain size d_{50} = 0.13 – 0.29mm. A mean value of 0.20mm was used for all calculations. A specific gravity s=2.6 was derived from geotechnical classification tests.

The bedform of the sand is also important and relevant for the scour assessment. The geophysical survey performed at the site showed a featureless seabed, with little or no local relief. This also suggested that the seabed was not highly dynamic. Hence, significant changes in seabed elevation due to sand migration were not anticipated.

Mobility due to currents

When currents are acting on a flat seabed, the sandy seabed material will be immobile until a certain threshold current velocity is reached. The Shields parameters θ, is defined in Equation 1.

$$\theta = \frac{(u^*)^2}{g(s-1)d_{50}} \tag{1}$$

Where u* is the bed shear velocity and g is the acceleration of gravity (9.81m/s²).

The critical value of the Shields parameter, θ_{cr}, is the value of the Shields parameter for which sediment motion is initiated. DNV [1] state that the critical value of the Shields parameter is θ_{cr} = 0.05 to 0.06. Alternatively, a formula dependent on grain size can be used [6]. For the example in this paper, this corresponds to a critical bed shear velocity u^*_{cr} of 0.013m/s.

The relationship between bed shear velocity u* and the depth averaged current velocity $\bar{U}$ is given in Equation 2 [6]

$$\frac{u^*}{\bar{U}} = \frac{1}{7} \cdot \left(\frac{d_{50}}{h}\right)^{1/7} \tag{2}$$

Where h is the water depth. The water depth at the site in this example is 30m. A critical depth averaged current velocity $\bar{U}_{cr}$ = 0.5m/s was thus calculated. This current speed is compared to the current data at the site in one of the subsequent sections.

Mobility due to waves

Waves in sufficiently shallow water (h < 10.H_s) produce an oscillatory velocity at seabed [6].

The wave-induced scour is primarily governed by the Keulegan-Carpenter number, KC in Equation 3 [1]

$$KC = \frac{u_{max} T_z}{D} \tag{3}$$

Where u_{max} is the maximum value of the orbital velocity, D is the pile diameter and T_z is the wave period. A wave period dependent on H_s was used for the calculations.

A graph of KC vs. significant wave height, H_s is shown in Figure 1 for 30.0m water depth. DNV [1] state that for KC < 6, no scour hole is formed. The chart shows that H_s must exceed 8m before wave-induced scour takes place.

Figure 1 – KC vs. H_s for 30m water depth

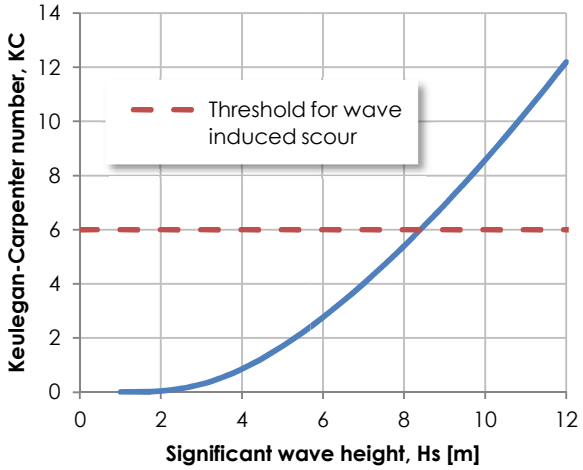

METOCEAN DATA

Current

Insight into the current regime is provided directly by field data measurements. Currents have been measured since 2003 at

the FINO1 platform, which is located in the vicinity of the site considered in this paper. The current speeds and directions collected during a 2.5 year period are described by Herklotz [7]. The current measurements at 8m water depth are shown in Figure 2. The water depth at the example location is nearly identical to the water depth at FINO1. The orange line at the bottom of the figure represents the current speed, the black line the current direction.

Figure 2 – 2005 current statistics at 8m water depth for FINO1 [7]

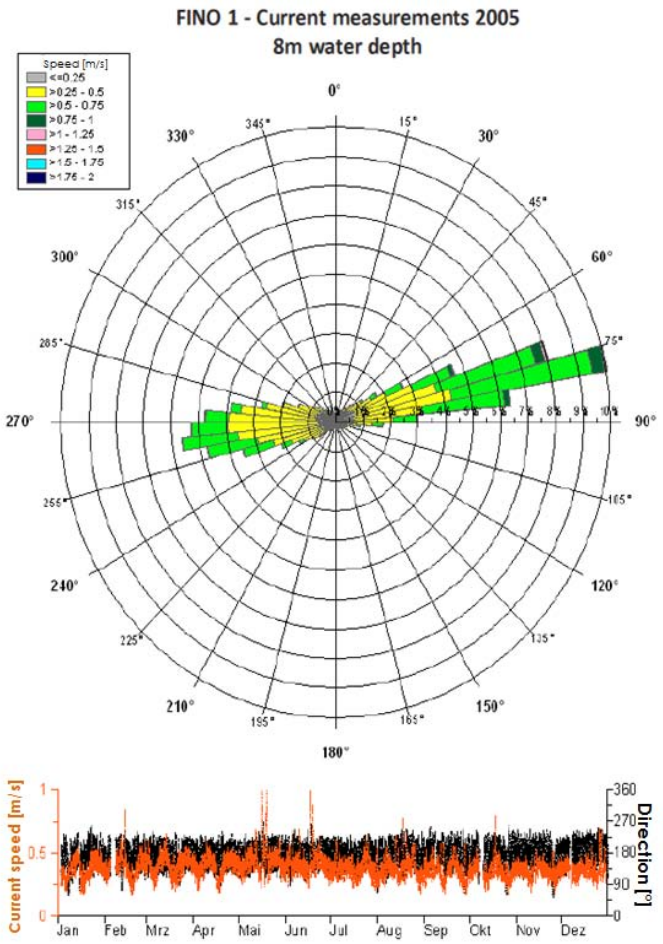

In order to provide input for the model for scour development with time, a sine-wave was fitted to the peaks of the current velocity at 8m depth as shown in Figure 3. The sinusoidal fit corresponding to the spring tide/neap tide cycle is shown in yellow. An average current velocity of 0.4m/s in combination with an amplitude of 0.2m/s fits the data well.

Figure 3 – Sinusoidal fit to current data at 8m water depth for FINO1

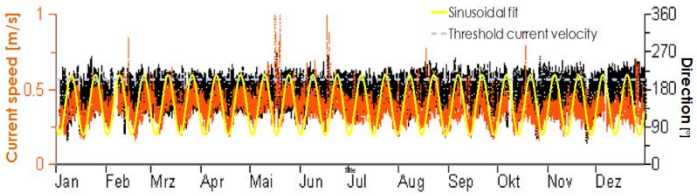

Waves

The wave climate was also measured at FINO1. The waves measured during the storm "Tilo" are described in [8] (Figure 4). The chart shows that during the extreme storm, the significant wave height exceeded 8m during a period of approximately 1 hour. Figure 1 suggests therefore that wave-induced scour will therefore be limited during the lifetime of the wind turbine foundations.

Figure 4 – Significant wave heights measured at FINO1 during storm "Tilo", November 2007 [8]

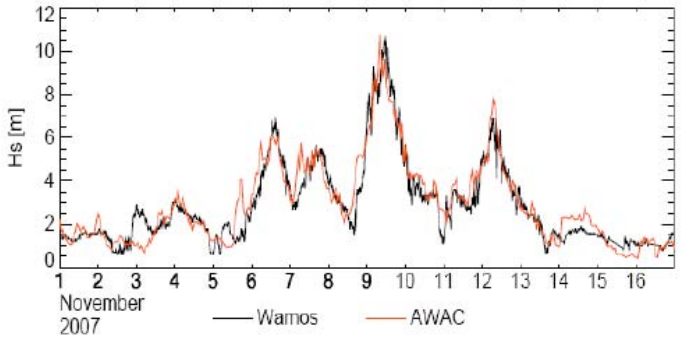

SCOUR CALCULATIONS

Equilibrium scour depth for single piles

The equilibrium local scour depth, S_{eq}, is given by DNV [1] for a single cylindrical pile as the expression in Equation 4. The relative importance of the current and waves is governed by the Keulegan-Carpenter number KC.

$$\frac{S_{eq}}{D} = 1.3\left\{1 - \exp\left[-0.03\left(KC - 6\right)\right]\right\} \qquad (4)$$

This formula predicts no scour when KC < 0. However, DNV state that for steady current KC→∞. In this case the equilibrium scour depth is 1.3D. Several other formulations exist but these all refer back to the equilibrium scour depth of 1.3D for steady current conditions. Note that for large diameter piles, this formula must be used with caution [1].

The scour depth in steady current conditions is given by Whitehouse [9] in Equation 5 based on the Shields parameter θ. Equation 5 is based on scale model tests [9].

$$\frac{S_{eq}}{D} = 1.3 \quad \text{when} \; \theta \geq \theta_{cr}$$
$$\frac{S_{eq}}{D} = 1.3\left[2\sqrt{\frac{\theta}{\theta_{cr}} - 1.0}\right] \quad \text{when} \; 0.25 \leq \frac{\theta}{\theta_{cr}} < 1 \tag{5}$$

When $\theta/\theta_{cr}<0.25$, there is no scour. Figure 5 shows the variation of scour depth with flow speed for the scale model tests.

Figure 5 – Variation of scour depth with flow speed [9]

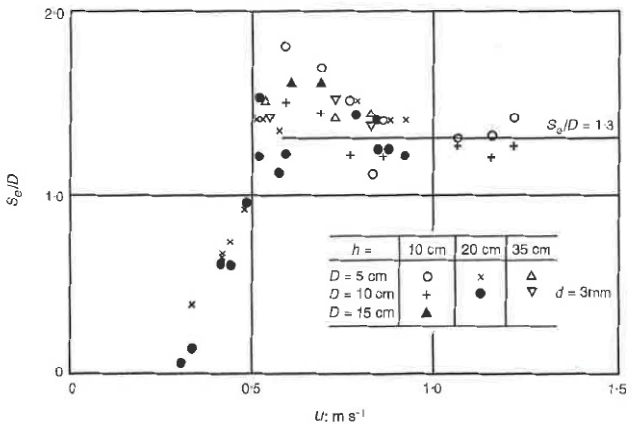

Time scale of scour development for single piles

Scour will only start to develop when the currents and/or waves are intense enough to cause seabed mobility. In current dominated conditions, scour can take months or years to develop. In wave dominated conditions, equilibrium is reached relatively quickly (order of magnitude of a few hours).

Scour development is not a steady process. The current data in Figure 3 shows that the threshold current velocity is only exceeded during peaks of tidal current velocity. Also, wave-induced scour will only develop during extreme storms as shown in Figure 1.

The characteristic time scale of local scour around single piles as well as a formula for scour development in current-dominated conditions is given in [1] and [10]. Equation 6 shows the formula for scour development while the characteristic time scale, T_{char}, is given in Equation 7.

$$S(t) = S_{eq}\left[1 - \exp\left(-\frac{t}{T_{char}}\right)\right] \tag{6}$$

$$T^* = A\theta^B$$
$$T_{char} = \frac{T^* D^2}{\sqrt{g(s-1)d_{50}^3}} \tag{7}$$

A and B are calibration parameters which were determined to be A = 0.014 and B = -1.29 [10].

Hindcasting method for single pile scour

Rudolph et al [11] propose a scheme for hindcasting of local scour development based on available metocean data. A given period of time is split up into a number of time increments, Δt (Δt equals the resolution of the metocean data), and for each time increment, the current speed, water depth and wave orbital velocity is computed. Based on the properties of the bed material and the hydrodynamic parameters, the equilibrium scour depth and characteristic scour depth can be determined for each time step.

For current dominated conditions, the equilibrium scour depth is computed according to Equation 5 and the characteristic time scale is given by Equation 7. For each time step, the computed equilibrium scour depth is compared to the scour depth at the end of the previous time increment (S_n). If the equilibrium scour depth ($S_{eq,n+1}$) is larger than the scour depth for the previous time increment, scour is allowed to develop according to Equation 8. If the equilibrium scour depth is smaller than the scour that has already developed, the scour depth remains constant. The process of back-filling of the scour hole is therefore ignored. This is a conservative assumption which can be justified at locations where large-scale sediment transport is not observed.

$$S_{n+1} = S_n + \Delta S(t)$$
$$\Delta S(t) = S_{eq,n+1}\left[1 - \exp\left(-\frac{\Delta t}{T_{char,n+1}}\right)\right] \quad \text{if} \; S_{eq,n+1} > S_n \tag{8}$$

Detailed numerical data of the hydrodynamic parameters (current velocity, significant wave height and water depth) was not available at the windfarm site under consideration. Therefore, an indicative simulation of the scour development was performed using the sinusoidal fit to the current data from Figure 3. Equation 8 is applied to the sinusoidal time series and the calculated evolution of scour depth is presented in Figure 6. In this example, the pile diameter D=2.5m.

The sensitivity to the grain size was also checked using a low estimate d_{50} = 0.13mm, a best estimate d_{50} = 0.20mm and a high estimate d_{50} = 0.29mm. In all cases, an equilibrium scour depth of 3.25m is reached. For the best estimate grain size, the scour hole reaches and equilibrium depth after approximately 200 days. For the low estimate grain size, the scour development takes approximately 20% more time. The scour development for the high estimate grain size is ~15% quicker.

Note that only current-induced scour was considered in this calculation due to the relatively deep water at the wind farm site.

Figure 6 – Prediction of scour depth development based on sinusoidal fit to current velocity

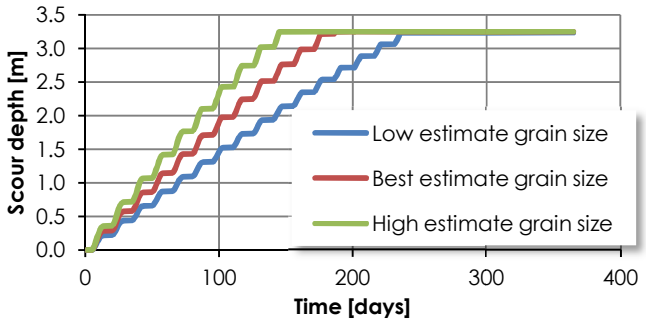

Global scour

Global scour (also called dishpan scour) is caused by the change in flow velocity and turbulence due to the close proximity of several piles and/or other structural elements. For engineering design, global scour is assumed to consist of an overall lowering of the seabed around the entire structure which in turn reduces the effective vertical stress around the piles. Global scour also increases the depth where no lateral resistance is considered. However, axial pile capacity is particularly affected by loss of vertical stress around the pile and therefore global scour is assessed accounting for the average stress reduction that is appropriate for a given structure. Scour induced by the presence of structural elements near the seabed does not necessarily result in general seabed lowering but can contribute to the reduction in vertical effective stress. Therefore, global scour is a means by which the average effect of local scour can be accounted for, as well as a method for dealing with general lowering of the seabed.

For this study, global scour has been considered to arise from the following sources:

- Effect of turbulence and scour induced by multiple piles;
- Effect of tripod bracing and central column;
- Effect of seabed sediment mobility.

Scour due to the interaction of multiple piles is well documented [10] and can be quantified based on experimental data for pile groups although test data for the scour development around three piles in a triangular configuration in current-dominated conditions is not published to date.

The effect of foundation bottom struts (bracing) can be treated as a horizontal tubular member (using methods developed for spanning pipelines) with a certain offset from the seabed. Nevertheless, these phenomena are not documented extensively in the literature and therefore, predictions will be much less accurate than the predictions for single pile scour.

Seabed sediment mobility appears to be limited (no sand waves or obvious bedforms). Therefore, no quantification of general seabed lowering has been attempted.

However, uncertainty about the possibility of seabed lowering can be considered implicitly in the selection of a conservative global scour value for design.

SCOUR PREDICTIONS VS. FIELD MEASUREMENTS

Tripod piles

Scour was measured around the tripod piles at location AV7 of Park Alpha Ventus (PAV) with echosounders and through a bathymetric survey [2]. A drawing of the tripod foundations used at Alpha Ventus is shown in Figure 7.

Figure 7 – Tripod foundation used at Park Alpha Ventus [2]

Fixed echosounders were placed along the pile sleeves and underneath the central column. The scour measurements from this test field provided a means to validate the methodology outlined in this paper. The measured and the predicted scour depth around the piles are plotted in Figure 8. The wave climate measured at the site is also plotted for information. Red dashed lines represent extreme storm events.

The figure shows that the predictions agree very well with the measured data. As predicted, the scour around the tripod piles reaches an equilibrium depth of approximately 3.0-3.5m between 150-200 days after installation. It should also be noted that scour depth is not uniform around the tripod pile. Scour is most severe at the sensor ES 6 which is most exposed to the dominating current direction.

The data shows no clear correlation between storm periods and scour depth. No notable increase in the scour depth is measured during periods with high significant wave height. The severest storms occurred after reaching equilibrium scour depth, notable increase were therefore not expected.

It should be noted that at the end of August 2010 and the end of October 2010, there is a sudden change in the measured scour depth. It is not clear whether this sudden change corresponds to sudden change in the scour depth or whether it is due to equipment malfunctioning.

Central column of tripod foundations

Scour below the central column was also measured with echosounders [2]. The measured scour depth is plotted in Figure 9. The wave climate measured at the site is again plotted for information.

Figure 8 – Comparison of measured and predicted scour depth around tripod piles (measurement data from [2])

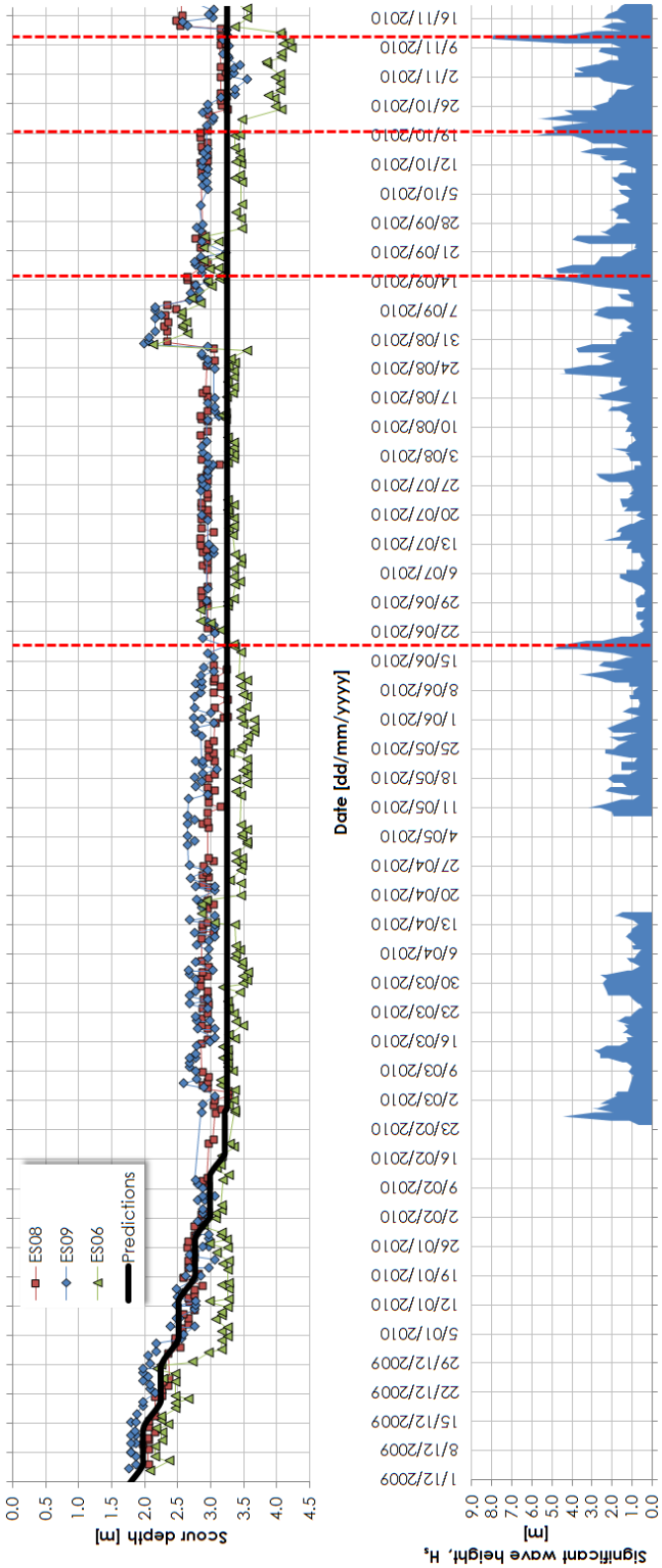

Figure 9 – Measured scour depth below the central tripod column (measurement data from [2])

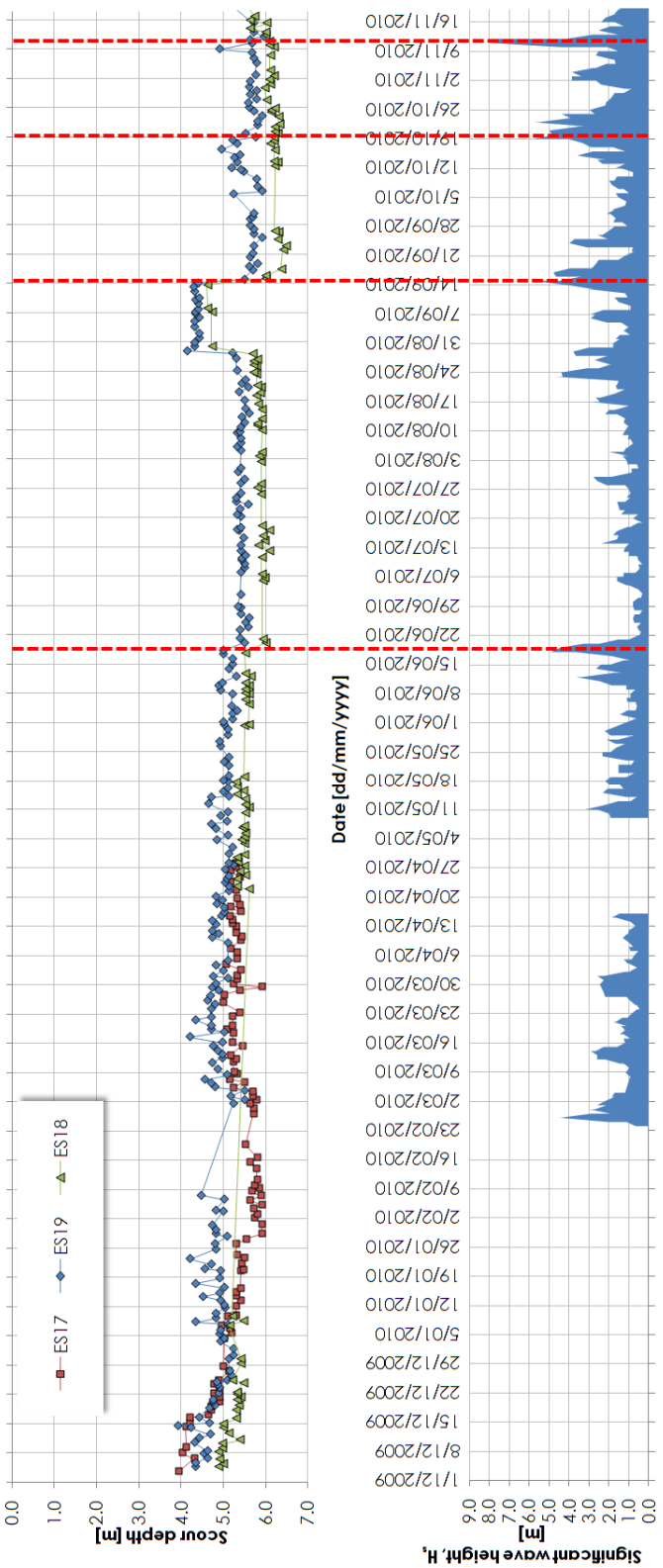

The data show that there is no steady-state scour depth reached for the central column. Most of the scour has developed during the first 4-5 months after installation. Afterwards, scour continues to increase slowly at a rate of approximately 1m/yr from 5.0m at the start of 2010 to 6.0m at the end of 2010. The scour below the central column does not yet seem to have an influence on the scour around the tripod piles as shown in [2].

Comparison with the wave data shows that there seems to be a correlation between periods of extreme weather and scour development below the central column. This might be due to the central column being open at the bottom leading to significant pumping action in periods with high waves. These pumping effects were also shown in model tests documented in [12]. However, equipment malfunctioning cannot be ruled out either. Pumping effects could be avoided on future projects by fitting flow diverters, which ensure water flows out horizontally rather than vertically, to the bottom of the tripod central column.

EFFECT OF SCOUR ON PILE CAPACITY

One of the main impacts of scour for pile capacity is to reduce the vertical effective stress and therefore the radial stress on the piles which governs the shaft resistance. For this reason, the effect of scour on effective stress reduction is evaluated.

Lateral extent of scour holes

In order to model the actual scour shape in a finite element model, the lateral extent of local scour holes should be determined. DNV [1] recommends that the lateral extent can be calculated according to Equation 9:

$$r = \frac{D}{2} + \frac{S_{eq}}{\tan\varphi} \tag{9}$$

Where r is the radius of the scour hole and φ is the angle of repose of the soil. [13] mentions that the angle on the downstream side is equal to 1/2 to 2/3 of the internal friction angle, φ', of the sand. On the upstream side, the angle is larger. Assuming φ' = 37.5°, the angle of repose (2/3φ') would be φ = 25°. The analyses presented in this paper are for an angle of repose of 2/3φ'. The seems to be in line with the multibeam survey results presented in [2]. More detailed analysis is possible where the effect of waves and currents on the submarine slope stability is studied [14] but this is beyond the scope of this paper.

The lateral extent of the scour holes around the foundation piles and under the central column is shown in Figure 10 assuming 5.0m scour under the central column, and an equilibrium scour depth of 3.2m for the piles.

Figure 10 – Extent of scour holes around tripod piles

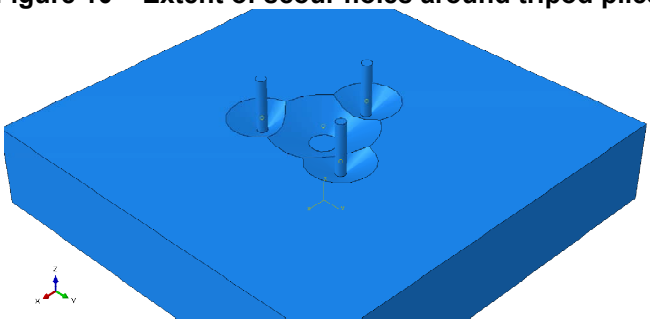

The figure shows that the local scour holes would interact to some extent with the scour hole below the central column. However, the seabed lowering due to scour below the central column does not extend to the location of the piles. The effect of the different local scour holes on the vertical effective stress is investigated in the subsequent section.

Influence of local scour holes around piles

A linear elastic finite element model was set up in Abaqus to quantify the reduction in effective stress due to the presence of local scour holes. The soil was model as a linear elastic material with a Young's modulus of E' = 100GPa, a Poisson's ratio, v' = 0.3 and an effective unit weight of $\gamma' = 10kN/m^3$.

A local scour hole with a depth of 3.2m, a radius of 8.1m and 25° side slopes was modelled to obtain the vertical effective stress around the pile after scouring. A contour plot of the vertical effective stress is shown in Figure 11.

The effect of the scour hole on the vertical effective stress at the location of the pile-soil interface is shown in Figure 12. Since there is no soil present, the vertical effective stress is zero down to the equilibrium scour depth. At greater depths, an overburden recovery zone exists where the vertical effective stress increases back to the undisturbed value. This is in accordance with the recommendations given in [5].

Figure 11 – Vertical effective stress due to local scour around tripod piles

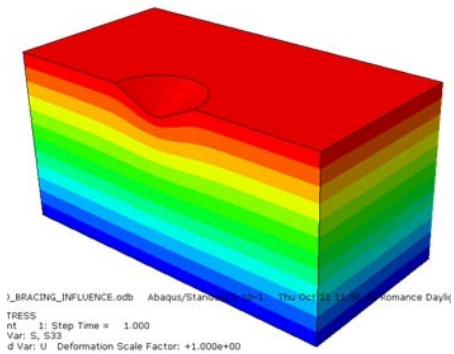

Figure 12 – Vertical effective stress profiles due to local scour around tripod piles

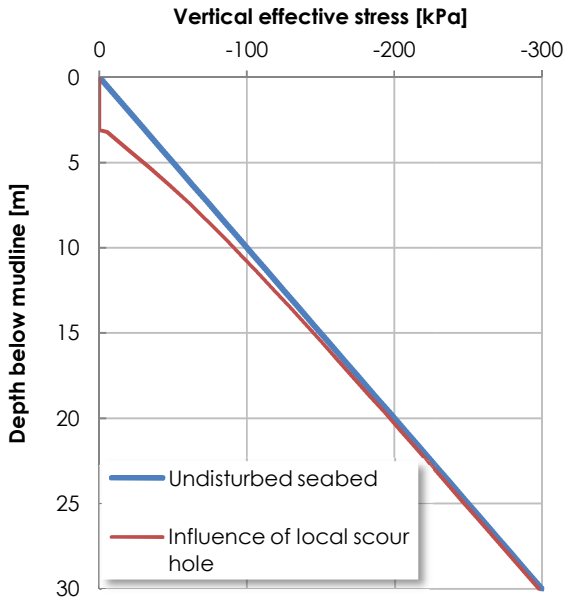

Influence of bracings

The scour hole below the bracing was modeled as a channel with a bottom width equal to the largest bracing diameter (B = 3.82m), a depth of 1.7m and side slopes of 25°. The depth of this channel was obtained by considering an analogy with a free-spanning pipeline. A contour plot of the vertical effective stress in the model is shown in Figure 13.

The effect of the bracing scour channel on the vertical effective stress at the pile-soil interface is shown in Figure 14. The figure shows the vertical effective stress at three locations:

- Pile-soil interface facing the bracing channel (0°);
- Pile-soil interface on the opposite side of the bracing channel (180°);
- Pile-soil interface between the two previous locations (90°).

Figure 13 – Vertical effective stress due to local scour around tripod piles and bracing

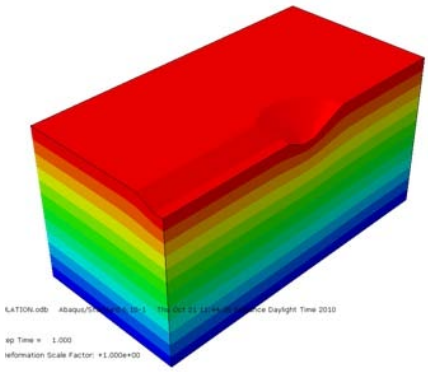

Figure 14 – Vertical effective stress profiles due to local scour around tripod piles and bracing

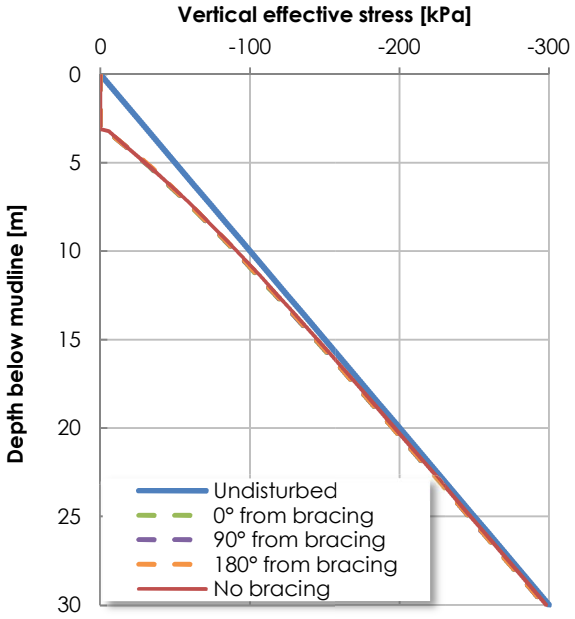

The vertical effective stress for an undisturbed seabed is also shown for information.

Figure 14 shows that the influence of the bracing channel on the vertical effective stress is negligible compared to the influence of the local scour hole. Therefore, it is not necessary to consider the component of global scour due to the bracings.

Influence of central scour hole

Even though a flow diverter might be fitted below the central column of the tripods, the effect of possibly having 5.0m of scour below the central column was analyzed to quantify the reduction in vertical stress and therefore how much global scour is needed to account for the central scour, should it occurs.

The scour below the central column was modeled as a hole with a depth of 5.0m, a radius of 13.0m and 25° side slopes. Figure 10 shows that the scour hole below the central column overlaps to a certain extent with the local scour holes around the tripod piles.

The contour plot of vertical effective stress is shown in Figure 15. The figure shows that the central column will cause a reduction of the vertical effective stress which will also influence the tripod piles to some extent.

The vertical effective stress around the tripod piles is shown in Figure 16, and was again quantified at three locations:

- Pile-soil interface facing the central column (0°);
- Pile-soil interface on the opposite side of the central column (180°);
- Pile-soil interface between the two previous locations (90°).

Figure 15 – Vertical effective stress due to local scour around tripod piles and central column

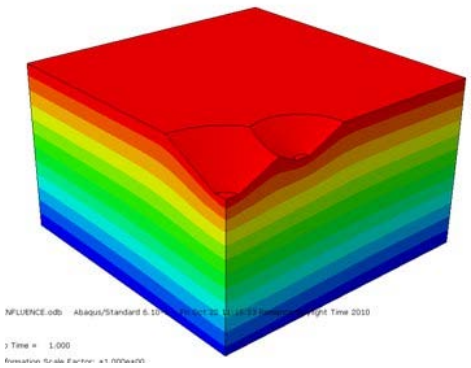

Figure 16 – Vertical effective stress profiles due to local scour around tripod piles and central column

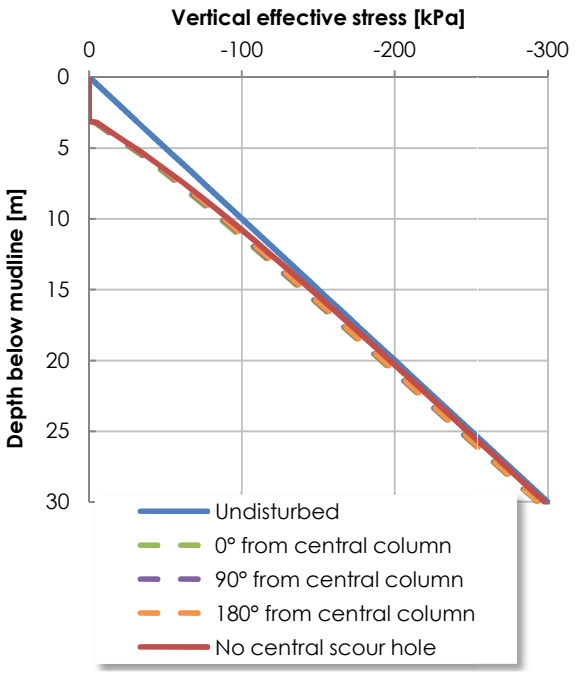

The effective stress profile without the influence of the central column is also shown in Figure 16. The figure shows that the central scour hole would cause a higher reduction in vertical effective stress than the tripod bracings. A component of global scour should therefore be considered to account for this reduction.

Summary

The influence of local scour around the piles and scour below the bracings and central column was quantified with a linear elastic finite element model, in order to understand the change of the vertical effective stress at the pile location. The different scour holes were modeled explicitly and the vertical effective stress at the pile-soil interface was determined at different locations around the circumference of the pile. The results of the different contributions are shown in Figure 17 which indicates that vertical effective stress reductions of less than 2kPa are likely to be caused by bracing and central column scour.

The combination of 3.2m of local scour around the tripod piles in combination with 5.0m below the central column causes the highest reduction in vertical effective stress. However, if the flow diverters are fitted below the central column, the development of 5.0m of scour below the central column is unlikely.

Therefore, considering possible contributions to scour below the tripod from hydrodynamic interaction between piles, the effect of scour below the tripod bracing and central column, and making an allowance for sediment mobility and seabed level change, a global scour depth of 0.8m is proposed. Figure 17 shows that the design profile according of vertical effective stress derived according to [5] (3.2m local scour plus 0.8m global) provides a sufficient safety margin, even for the case with a 5.0m deep scour hole below the central column.

Figure 17 – Vertical effective stress due to local scour and global scour with design profile

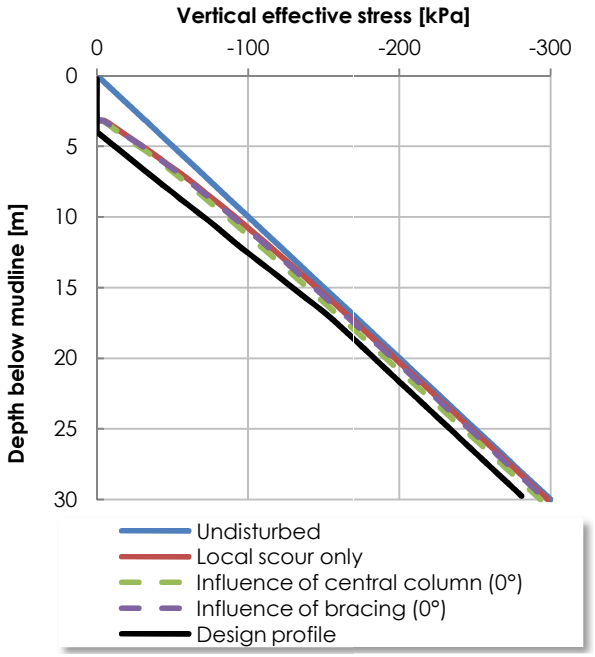

CONCLUSIONS

A scour depth prediction model was established in this paper. The prediction model was based on the work by [10] and [11]. The model predictions were compared to the scour depth measurements at windfarm site Park Alpha Ventus (PAV) [2].

Scour around the foundation piles is expected to reach equilibrium after approximately 175 days and the local scour depth is not expected to exceed 1.3 times the pile diameter (i.e. 3.2m) based on both model predictions and measurements at PAV.

Other causes of scour, such as pile-pile interaction, effect of proximity of bracing and central column to the seabed, and seabed mobility were also assessed in order to determine the amount of global scour to be considered. The pile-pile scour is expected to be much less than 0.8m while the proximity of the bracing has the largest effect theoretically with local scour on the order of 1.5m. At PAV, about 5.0m scour was measured below the central column but this is not expected to occur if the fitting of a flow diverter is fitted to the bottom of the column. Moreover, the measured maximum scour (3.3m) around the piles at PAV includes all scour effects.

The effect of scour on the vertical effective stress around the tripod piles was assessed with a linear elastic finite element model. Local scour has an important effect while scour below the bracing and central column a much more limited effect. Should up to 5m scour below the central column occur, the effective stress reduction would be equivalent to approximately 0.2m of global scour. Therefore, considering the combined effects of multiple pile interaction, possible scour below the central column, and making an allowance for seabed mobility, a global scour depth of 0.8m is recommended.

This global scour allowance provides an additional margin where the pile is assumed unsupported laterally.

Scour around the tripods should be monitored periodically and if scour exceeds the design values, the impact on pile stability and stiffness should be assessed to determine if scour remedial measures are needed.

REFERENCES

[1] DNV-OS-J101, *DNV-OS-J101 - Design of offshore wind turbine structures*. Det Norske Veritas, 2010.

[2] M. Lambers-Huesmann and M. Zeiler, “Untersuchungen zur Kolkentwicklung und Kolkdynamik im Testfeld Alpha Ventus,” in *Veroffentlichungen des Grundbauinstitutes der Technischen Universitat Berlin Heft Nr. 56*, Berlin, 2011.

[3] PwC, “Offshore proof Turning windpower promise into performance,” PwC offshore windpower survey – based on field research conducted by GBI, 2011.

[4] DECC, “Dynamics of scour pits and scour protection - Synthesis report and recommendations (Milestones 2 and 3),” The Department of Energy and Climate Change, 2008.

[5] API RP GEO, “API RP2 GEO Geotechnical and Foundation Design Considerations,” 2011.

[6] R. Soulsby, “Dynamics of Marine Sands,” Thomas Telford, 1997.

[7] K. Herklotz, “Oceanographic Results of Two Years Operation of the First Offshore Wind Research Platform in the German Bight - FINO1,” *DEWI Magazin*, vol. 30, 2007.

[8] O. Outzen, K. Herklotz, H. Heinrich, and C. Lefebvre, “Extreme Waves at FINO1 Research Platform Caused by Storm ‘Tilo’ on 9 November 2007,” *DEWI Magazin*, vol. 33, 2008.

[9] R. Whitehouse, *Scour at marine structures: A manual for practical applications*. Inst of Civil Engineers Pub, 1998.

[10] B. M. Sumer and J. Fredsøe, *The mechanics of scour in the marine environment*. World Scientific Publishing Company Incorporated, 2002.

[11] D. Rudolph, T. C. Raaijmakers, C. J. M. Stam, and W. Op den Velde, “Evaluation of scour development around offshore monopiles based on measurements in the Q7 windpark,” presented at the European Offshore Wind Conference, Berlin, 2007.

[12] A. Stahlmann and T. Schlurmann, “Physical Modeling of Scour around Tripod Foundation Structures for Offshore Wind Energy Converters,” *COASTAL ENGINEERING*, p. 2, 2010.

[13] M. Achmus, Y.-S. Kuo, and K. Abdel-Rahman, “Numerical Investigation of Scour Effect on Lateral Resistance of Windfarm Monopiles,” in *Proceedings of the Twentieth (2010) International Offshore and Polar Engineering Conference*, Beijing, China, 2010, pp. 619–623.

[14] J. Bubel and J. Grabe, “Stability of submarine foundation pits,” in *SUT OSIG*, London, 2012, pp. 347–354.